



Published as: *Nature*. 2007 June 7; 447(7145): 720–724.

## Dscam2 mediates axonal tiling in the *Drosophila* visual system

S. Sean Millard<sup>1</sup>, John J. Flanagan<sup>1</sup>, Kartik S. Pappu<sup>1</sup>, Wei Wu<sup>1</sup>, and S. Lawrence Zipursky<sup>1</sup>

<sup>1</sup>Howard Hughes Medical Institute, Department of Biological Chemistry, David Geffen School of Medicine, University of California, Los Angeles, Los Angeles, California 90095, USA.

### Abstract

Sensory processing centres in both the vertebrate and the invertebrate brain are often organized into reiterated columns, thus facilitating an internal topographic representation of the external world. Cells within each column are arranged in a stereotyped fashion and form precise patterns of synaptic connections within discrete layers. These connections are largely confined to a single column, thereby preserving the spatial information from the periphery. Other neurons integrate this information by connecting to multiple columns. Restricting axons to columns is conceptually similar to tiling. Axons and dendrites of neighbouring neurons of the same class use tiling to form complete, yet non-overlapping, receptive fields<sup>1-3</sup>. It is thought that, at the molecular level, cell-surface proteins mediate tiling through contact-dependent repulsive interactions<sup>1,2,4,5</sup>, but proteins serving this function have not yet been identified. Here we show that the immunoglobulin superfamily member Dscam2 restricts the connections formed by L1 lamina neurons to columns in the *Drosophila* visual system. Our data support a model in which Dscam2 homophilic interactions mediate repulsion between neurites of L1 cells in neighbouring columns. We propose that Dscam2 is a tiling receptor for L1 neurons.

The *Drosophila* visual system is a modular structure<sup>6,7</sup>. The retina contains 750 simple eyes, each containing eight photoreceptor neurons or R cells (R1–R8). R cells project into the brain, where they make connections within two neuropils, the lamina and medulla. R1–R6 neurons target to the lamina, where they form synapses with lamina neurons (L1–L5). R7, R8 and L1–L5 form connections in single columns within layers in the medulla, and each column contains one axon of each of these cell types. As a consequence of this wiring pattern, each column processes motion (lamina neurons) and colour (R7 and R8) from a single point in space<sup>6</sup>. Although some progress has been made in understanding how neurons select different layers within each of the 750 columns<sup>6</sup>, the molecular mechanisms that restrict synaptic connections to a single column are not known.

Dscam2 belongs to a conserved family of cell-surface proteins expressed in the nervous systems of many different organisms<sup>8-10</sup>. Down syndrome cell adhesion molecule (DSCAM) was originally identified as an open reading frame in a region of human chromosome 21 critical for Down's syndrome<sup>11</sup>. There are four *Dscam* genes in the fly genome (*Dscam*, and *Dscam2-4*). They encode type I transmembrane proteins that share about 30% sequence identity and have a common extracellular domain comprising ten

©2007 Nature Publishing Group

Correspondence and requests for materials should be addressed to S.L.Z. (lzipursky@mednet.ucla.edu).

**Full Methods** and any associated references are available in the online version of the paper at [www.nature.com/nature](http://www.nature.com/nature).

**Supplementary Information** is linked to the online version of the paper at [www.nature.com/nature](http://www.nature.com/nature).

Reprints and permissions information is available at [www.nature.com/reprints](http://www.nature.com/reprints). The Dscam2-4 sequences can be found in the NCBI database under accession numbers AE014296, AE003718 and AE003556, respectively.

The authors declare no competing financial interests.

immunoglobulin and six fibronectin type III repeats (Fig. 1a). These proteins have divergent cytoplasmic tails. The genomic organization of each fly *Dscam* family member differs considerably. *Dscam* encodes four cassettes of alternative exons that can potentially generate 38,016 different proteins through mutually exclusive alternative splicing<sup>12</sup>. *Dscam* has a function in forming neural circuits throughout the fly brain<sup>12-17</sup>. *Dscam* isoforms bind homophilically<sup>18</sup>, and *in vivo* studies indicate that these interactions promote repulsion<sup>18-21</sup>. *Dscam2-4* do not show extensive isoform diversity, and in this way these family members are more similar to mammalian DSCAMs. *Dscam2* has two alternative immunoglobulin 7 domains that share about 50% sequence identity and are referred to as *Dscam2A* and *Dscam2B*. Given the structural similarities between *Dscam* and *Dscam2* and the prominent expression of *Dscam2* on neurites in the developing brain (see Fig. 1d), we proposed that interactions between *Dscam2* proteins are required for patterning neuronal connections.

To assess the function of *Dscam2*, we generated protein-null mutations in the gene by homologous recombination<sup>22</sup> (Fig. 1b-e; see Methods). The *Dscam2* mutants were viable but had marked defects in R-cell projections into the medulla (Fig. 1f, g). Using a panel of cell-type specific markers in the medulla (Supplementary Fig. 1), we observed widespread defects in axonal and dendritic organization. As wiring defects in one class of neurons may indirectly affect other classes, it was not possible to accurately assess the function of *Dscam2* in homozygous mutant animals.

To identify a specific cell type that requires *Dscam2*, we removed it from subsets of neurons by using genetic mosaic techniques. We targeted four cell types (R7, R8, L1 and L2) that connect to specific layers within each medulla column (Fig. 2a). To assess whether *Dscam2* was required in R7 and R8, genetically mosaic animals were generated in which mutant R7 and R8 cells projected into an otherwise wild-type brain. R7 ( $n = 87$ ) and R8 neurons ( $n = 336$ ; see Methods) lacking *Dscam2* formed patterns of projections that were indistinguishable from their wild-type counterparts (Fig. 2b, c).

We extended our analysis to a subset of lamina neurons, L1 and L2. L1 axons arborize in two medulla layers, m1 and m5. In contrast, L2 axons form a single terminal arborization at the m2 layer. To assess whether *Dscam2* is required in L1 and L2 neurons, we generated single mutant cells in an otherwise wild-type background, using the MARCM technique<sup>23</sup>. To do this, we expressed FLP recombinase under the control of a *Dachshund* (*Dac*) enhancer<sup>24</sup> (see Methods) to induce recombination selectively in lamina precursor cells just before their final cell division (Fig. 2d). In wild-type controls, fewer than ten lamina neurons were labelled per optic lobe. Of these, 90% were L1 neurons and 10% were L2. Wild-type L1 (Fig. 2g;  $n = 165$ ) and L2 (Fig. 2e;  $n = 28$ ) cells arborized in the correct layers and were restricted to a single column. Other lamina neurons were not labelled by this procedure (see Methods).

*Dscam2* mutant L1 neurons arborized in the correct layers. These arbors, however, were no longer restricted to a single column (67%;  $n = 228$ ) and often extended over several columnar units (Fig. 2h, i). These neurons formed terminal structures within the appropriate layers in adjacent columns. Phenotypes were observed in m1, in m5 or in both of these layers. In some cases (less than 10%) L1 axons bifurcated between m1 and m5 and each branch targeted to the appropriate layer in adjacent columns (see Supplementary Fig. 2). In marked contrast to mutant L1 neurons, the terminal arbors of mutant L2 neurons were indistinguishable from the wild type (Fig. 2e, f;  $n = 97$ ). In summary, *Dscam2* is required within L1 neurons to restrict arbors to a single column. Conversely, R7, R8 and L2 axons are restricted to a single column by *Dscam2*-independent mechanisms.

How might *Dscam2* restrict L1 processes to a single column? Columnar restriction in the medulla is reminiscent of dendritic tiling<sup>25</sup>. Here dendrites of neighbouring cells of the same class do not overlap. Although the molecular mechanisms underlying tiling are not known, it has been proposed that they involve homotypic repulsion between cells of the same type<sup>4</sup>. If *Dscam2* restricts L1 processes in this manner then we would predict, first, that *Dscam2* would exhibit homophilic binding; second, that L1 processes expressing *Dscam2* would contact each other during development and then retract to a single column; and third, that wild-type L1 axonal processes would extend into adjacent columns in which L1 neurons were *Dscam2* mutant.

To assess whether *Dscam2* exhibits homophilic binding, we used cell aggregation assays and pull-down experiments as described previously for *Dscam18,19*. Two S2 cell populations expressing different *Dscam2* isoforms (*Dscam2A* and *Dscam2B*) segregated into isoform-specific clusters (Fig. 3a, b). Similar results were obtained from mixing experiments between *Dscam2* and either *Dscam* or *Dscam3* (data not shown). Confirming this binding specificity, *Dscam2* ecto-domains fused to human Fc bound only to the full-length *Dscam2* proteins with the identical ectodomain (Fig. 3c, d). In summary, *Dscam2* interacts with itself in an isoform-specific manner and does not bind to other *Dscam* family members.

To assess whether L1 processes contact each other during development and whether *Dscam2* is expressed in these layers, we examined wild-type L1 arborization patterns and *Dscam2* antibody staining during pupal development. Using MARCM to label L1 cells, we observed growth cone expansions and immature interstitial branches at 30 h after puparium formation (APF) (Fig. 3e). About 10 h later, m1 and m5 arbors were exuberant, not restricted to columns, and neurites from neighbouring labelled cells contacted each other (Fig. 3f). During subsequent development these processes retracted and were restricted to a single column by 70 h APF (Fig. 3g). *Dscam2* was expressed within these layers throughout this time course. Expression peaked at 40 h APF and was markedly reduced by 70 h APF, by which time L1 arbors were restricted to a single column (Fig. 3h-j). It is not possible to determine which cells within these two layers account for the *Dscam2* immunoreactivity; however, the results of our genetic studies make it likely that minimally, L1 processes are *Dscam2* positive. *Dscam2* is also found in other layers, but at only low levels or not at all in R7 and R8 growth cones (Fig. 3j).

If L1 axons are restricted to a single column by *Dscam2* homophilic interactions, then wild-type L1 arbors should display a phenotype when they contact mutant axons lacking *Dscam2*. To address this, we used reverse MARCM<sup>26</sup>. As with MARCM, both wild-type and mutant lamina neurons are generated, but in reverse MARCM only the wild-type cells are labelled (Fig. 4a). As the frequency of generating labelled cells is low, the likelihood that a labelled wild-type L1 axon and a mutant lamina axon will be present in the same or an adjacent column is correspondingly low. In control experiments, labelled wild-type cells were restricted to columns in a wild-type genetic background (Fig. 4b;  $n = 444$ ). In contrast, of 466 wild-type L1 neurons examined using reverse MARCM, we observed 15 neurons extending processes into adjacent columns (Fig. 4c-e). Thus, *Dscam2* homophilic interactions are required for restricting L1 arbors to columns.

As both L1 and L2 mutant neurons are generated by *Dac-FLP* induced MARCM (see above), *Dscam2* could restrict L1 arbors either through repulsive interactions between L1 axons in adjacent columns or through adhesive interactions between L1 and L2 axons in the same column. Interactions with L2 axons are unlikely for two reasons: first, although L2 axons extend through the m1 layer, and thus could mediate interactions with L1 processes in this layer, they do not extend to the m5 layer, and second, the reverse MARCM phenotype is

exclusively asymmetric, suggesting that the mutant axon resides in an adjacent column (Fig. 4f, and Supplementary Fig. 2). In MARCM experiments, 61% of the mutant arbors extended in both directions, but under reverse MARCM conditions none of the phenotypes were bidirectional. These data argue that *Dscam2* mediates axonal tiling between L1 processes in neighbouring columns (Fig. 4f, g).

Columnar restriction is a common organizing principle used by many sensory systems that relay spatial information from the periphery to processing centres in the brain. As a result of the reiterative nature of these circuits, multiple targets are available in close proximity to each other within the same layer. Local repulsion between axonal processes of identical neurons in adjacent columns, which make connections with these targets, provides a developmental strategy for preserving the spatial information in each circuit. Here we show that *Dscam2* is a homophilic tiling receptor for L1 neurons. Axonal tiling ensures that synaptic connections are made exclusively with targets in a single column.

The functions of *Dscam* and *Dscam2* have intriguing similarities and differences. Although both promote homophilic repulsion between neurites, they do so in different cellular contexts. As each neuron expresses a unique set of *Dscam* isoforms, neurites from the same cell selectively recognize and repel each other<sup>17-21,27,28</sup>. This process, called ‘self avoidance’, facilitates the uniform coverage of synaptic fields in the nervous system<sup>14,19-21</sup>. By contrast, *Dscam2* mediates repulsive interactions between neurites of the same cell type. This process, called tiling, limits connections to a local area. Tiling and self avoidance therefore act in concert to pattern dendritic and axonal fields in the nervous system.

## METHODS SUMMARY

### MARCM and reverse MARCM experiments

To generate *Dscam2* mutant lamina neurons, we used a *Dac-FLP* source on chromosome II and labelled the mutant cells with *actin-Gal4*, *UAS-CD8GFP*. Only L1 and L2 lamina neurons were labelled using this scheme. Using a different *Dac-FLP* source and other Gal4 sources, and performing mitotic recombination on a different chromosome arm, clones in all lamina neurons can be generated with this system (A. Nern and S.L.Z., unpublished observations). Thus, it remains formally possible that our MARCM experiments generated some unlabelled mutant lamina neurons. For reverse MARCM, two copies of *Dac-FLP* were used to increase the frequency of mitotic recombination (see fly stocks in Methods). Again, L1 and L2 cells were preferentially labelled. Wild-type MARCM clones generated with two copies of *Dac-FLP* were used as controls for the reverse MARCM experiments. Control and experimental samples were coded, mixed together, and scored blindly to avoid any bias. All other experimental procedures are described in Methods.

## METHODS

### Fly stocks

The following stocks were used for ends-out homologous recombination (see below for a description of the method): ‘HR stock’, *w*; *P[70-ISce-1], 4P[70-FLP]*, *ScO/CyO* and ‘Tester stock’, *w*; *70-FLP* (constitutive); *TM2/TM6b*. The *Dscam2* mutant alleles generated by homologous recombination were designated as *Dscam2<sup>null-1</sup>*, *Dscam2<sup>null-2</sup>* and *Dscam2<sup>null-3</sup>* and were maintained over *TM6b*. Markers for C3 and T1 neurons were *568-Gal4* and *10-50-Gal4*, respectively. R7 MARCM was performed largely as previously described<sup>29</sup>. The stocks used were *GMRFLP*, *Dscam2<sup>null</sup>*, *FRT79/CyO:TM6b* and *PanR7-Gal4*, *UASN-synaptobrevinGFP/CyO*, *Gal80*, *FRT79/TM6b*. The stocks used for R8 mosaics were *ey3.5FLP*, *RpS17*, *arm-lacZ*, *FRT80B/TM6b* and *w*; *Rh6-lacZ/CyO*; *Dscam2<sup>null-3</sup>*,

FRT80B/TM6b. For lamina neuron-specific MARCM the stocks were *w*; *Dac-FLP/CyOKr-GFP*, *Dscam2<sup>null</sup>*, *FRT79/TM6b*, and *w*; *actin-Gal4*, *UAS-CD8GFP*, *Gal80*, *FRT79/TM6b* (gift from A. Nose). The stocks used for reverse MARCM were *Dac-FLP*, *Dac-FLP*, *FRT79/CyO:TM6b* and *w*; *actin-Gal4*, *UAS CD8GFP*, *Gal80*, *Dscam2<sup>null-1</sup>*, *FRT79/TM6b*.

### Homologous recombination

Ends-out homologous recombination was performed essentially as described<sup>22</sup>. In brief, an 'ends-out' targeting construct, pW37 *Dscam2*, was generated that contained the *white* gene, immediately flanked upstream and downstream by insulator sequences from pPelican vector, followed by 3.5-kb and 3.1-kb homologous arms lying upstream and downstream from exon1 of *Dscam2*, respectively. Four independent donor lines harbouring the targeting transgene were crossed to the HR stock described above. Progeny from this cross were heat-shocked for 1 h at 38 °C at 0–48 h of development. About 600 mosaic females from each donor line were crossed to the tester stock (above) and non-mosaic progeny were then backcrossed to the tester stock. Stocks were established from flies that lacked eye colour mosaicism and were analysed by PCR. Three of the 40 lines established from 'red-eyed' flies contained targeted insertions.

### Molecular verification of *Dscam2* targeting

DNA was extracted from homozygous viable candidate lines, and genomic PCR was performed. Primers annealing outside the *Dscam2* locus were used in combination with primers annealing within the deleted region in the same reaction (Fig. 1c). The lack of band from the deleted exon1 region indicated the presence of the targeted allele.

### Construction of a lamina neuron-specific FLP source

A 325-bp subfragment of 3EE<sup>390</sup> (ref. 24) was used to build a lamina-specific FLP transgene. A *NotI*–*Bam*HI fragment containing the entire FLP coding region and a simian virus 40 (SV40)-poly(A) tail from the UAS-FLP vector (gift from J. Duffy) was cloned into the *NotI*–*Bam*HI-digested pCasper-4. The 325-bp enhancer fragment was then added as an *Eco*RI fragment upstream of the FLP-SV40-PolyA sequence. Finally, an hsp70 minimal promoter was inserted as a *Kpn*I–*NotI* adaptor fragment between the lamina enhancer and the FLP coding region to generate the dac-lamina-FLP vector. This vector was injected, in accordance with standard protocols, to generate several independent transgenic fly lines.

### Histology

Immunohistochemistry was performed as described<sup>30</sup>. The rabbit polyclonal antibody raised against the *Dscam2* cytoplasmic domain was used at a 1:2,000 dilution for immunohistochemistry.

### Cell aggregation

To generate plasmids containing both a *Dscam* cDNA and a fluorescent marker, pIZGM was created by removing the OpIE2 promoter from pIZT (Invitrogen) and replacing it with the metallothionine inducible promoter, MtnA, from pRMHA3. pIZRM was created by replacing GFP in pIZGM with a PCR product containing RFP. *Dscam* and *Dscam3* were excised from pBluescript, filled in to create blunt ends, and cloned into pIZGM or pIZRM. *Dscam2* was excised from pOTB7, filled in to create blunt ends, and cloned into pIZGM or pIZRM. Aggregation assays were performed as described<sup>19</sup>.

### Pull-down assays

*Dscam2A*, *Dscam2B*, and *Dscam3* full-length were modified with two tandemly arrayed Flag or haemagglutinin tags. These were introduced into each construct by cloning annealed

oligonucleotides containing the epitope in frame with the cytoplasmic domains of each Dscam family member. Dscam2A–Fc and Dscam2B–Fc were generated as described previously for Dscam–Fc proteins<sup>18</sup>. These fusion proteins comprised the N-terminal nine immunoglobulin domains and a single FNIII repeat from Dscam2 followed by human FcH. Pull-down assays were performed as described<sup>18</sup>.

## Supplementary Material

Refer to Web version on PubMed Central for supplementary material.

## Acknowledgments

We thank E. DeRobertis, U. Banerjee, W. Grueber, I. Meinertzhagen, A. Sagasti and members of the Zipursky laboratory for comments on the manuscript; J. Clemens for identifying and characterizing the *Dscam* paralogs; D. Gunning for cloning *Dscam3* and *Dscam4*; G. Marden for providing unpublished reagents that allowed us to generate the *Dac-FLP* construct; and Y. Zhu and R. Imondi for identifying the two medulla neuron Gal4 lines used in this study. S.L.Z. is an investigator of the Howard Hughes Medical Institute. This work was also supported by the NIH (S.L.Z.). S.S.M. was supported by a Cellular Neurobiology training grant from the NIH.

## References

- Blackshaw SE, Nicholls JG, Parnas, I. Expanded receptive fields of cutaneous mechanoreceptor cells after single neurone deletion in leech central nervous system. *J. Physiol. (Lond.)*. 1982; 326:261–268. [PubMed: 7108791]
- Grueber WB, Ye B, Moore AW, Jan LY, Jan YN. Dendrites of distinct classes of *Drosophila* sensory neurons show different capacities for homotypic repulsion. *Curr. Biol.* 2003; 13:618–626. [PubMed: 12699617]
- Sagasti A, Guido MR, Raible DW, Schier AF. Repulsive interactions shape the morphologies and functional arrangement of zebrafish peripheral sensory arbors. *Curr. Biol.* 2005; 15:804–814. [PubMed: 15886097]
- Jan YN, Jan LY. The control of dendrite development. *Neuron*. 2003; 40:229–242. [PubMed: 14556706]
- Kramer AP, Stent GS. Developmental arborization of sensory neurons in the leech *Haementeria ghilianii*. II. Experimentally induced variations in the branching pattern. *J. Neurosci.* 1985; 5:768–775. [PubMed: 3973696]
- Clandinin TR, Zipursky SL. Making connections in the fly visual system. *Neuron*. 2002; 35:827–841. [PubMed: 12372279]
- Meinertzhagen, IA.; Hanson Thomas, E. *The Development of Drosophila melanogaster*. Cold Spring Harbor Laboratory Press; New York: 1993.
- Barlow GM, Lyons GE, Richardson JA, Sarnat HB, Korenberg JR. DSCAM: an endogenous promoter drives expression in the developing CNS and neural crest. *Biochem. Biophys. Res. Commun.* 2002; 299:1–6. [PubMed: 12435380]
- Fusaoka E, Inoue T, Mineta K, Agata, K, Takeuchi K. Structure and function of primitive immunoglobulin superfamily neural cell adhesion molecules: a lesson from studies on planarian. *Genes Cells.* 2006; 11:541–555. [PubMed: 16629906]
- Graveley BR, et al. The organization and evolution of the dipteran and hymenopteran Down syndrome cell adhesion molecule (Dscam) genes. *RNA*. 2004; 10:1499–1506. [PubMed: 15383675]
- Yamakawa K, et al. DSCAM: a novel member of the immunoglobulin superfamily maps in a Down syndrome region and is involved in the development of the nervous system. *Hum. Mol. Genet.* 1998; 7:227–237. [PubMed: 9426258]
- Schmucker D, et al. *Drosophila* Dscam is an axon guidance receptor exhibiting extraordinary molecular diversity. *Cell*. 2000; 101:671–684. [PubMed: 10892653]
- Chen BE, et al. The molecular diversity of Dscam is functionally required for neuronal wiring specificity in *Drosophila*. *Cell*. 2006; 125:607–620. [PubMed: 16678102]

14. Hummel T, et al. Axonal targeting of olfactory receptor neurons in *Drosophila* is controlled by Dscam. *Neuron*. 2003; 37:221–231. [PubMed: 12546818]
15. Wang J, Zugates CT, Liang IH, Lee CH, Lee T. *Drosophila* Dscam is required for divergent segregation of sister branches and suppresses ectopic bifurcation of axons. *Neuron*. 2002; 33:559–571. [PubMed: 11856530]
16. Zhu H, et al. Dendritic patterning by Dscam and synaptic partner matching in the *Drosophila* antennal lobe. *Nature Neurosci*. 2006; 9:349–355. [PubMed: 16474389]
17. Zipursky SL, Wojtowicz WM, Hattori D. Got diversity? Wiring the fly brain with Dscam. *Trends Biochem. Sci*. 2006; 31:581–588. [PubMed: 16919957]
18. Wojtowicz WM, Flanagan JJ, Millard SS, Zipursky SL, Clemens JC. Alternative splicing of *Drosophila* Dscam generates axon guidance receptors that exhibit isoform-specific homophilic binding. *Cell*. 2004; 118:619–633. [PubMed: 15339666]
19. Matthews BJ, et al. Dendrite self-avoidance is controlled by Dscam. *Cell*. 2007; 129:593–604. [PubMed: 17482551]
20. Hughes ME, et al. Homophilic Dscam interactions control complex dendrite morphology. *Neuron*. 2007; 54:417–427. [PubMed: 17481395]
21. Soba P, et al. *Drosophila* sensory neurons require Dscam for dendritic self-avoidance and proper dendritic field organization. *Neuron*. 2007; 54:403–416. [PubMed: 17481394]
22. Gong WJ, Golic KG. Ends-out, or replacement, gene targeting in *Drosophila*. *Proc. Natl Acad. Sci. USA*. 2003; 100:2556–2561. [PubMed: 12589026]
23. Lee T, Luo L. Mosaic analysis with a repressible cell marker for studies of gene function in neuronal morphogenesis. *Neuron*. 1999; 22:451–461. [PubMed: 10197526]
24. Pappu KS, et al. Dual regulation and redundant function of two eye-specific enhancers of the *Drosophila* retinal determination gene dachshund. *Development*. 2005; 132:2895–2905. [PubMed: 15930118]
25. Grueber WB, Jan LY, Jan YN. Tiling of the *Drosophila* epidermis by multidendritic sensory neurons. *Development*. 2002; 129:2867–2878. [PubMed: 12050135]
26. Lee T, Winter C, Marticke SS, Lee A, Luo L. Essential roles of *Drosophila* RhoA in the regulation of neuroblast proliferation and dendritic but not axonal morphogenesis. *Neuron*. 2000; 25:307–316. [PubMed: 10719887]
27. Zhan XL, et al. Analysis of Dscam diversity in regulating axon guidance in *Drosophila* mushroom bodies. *Neuron*. 2004; 43:673–686. [PubMed: 15339649]
28. Neves G, Zucker J, Daly M, Chess A. Stochastic yet biased expression of multiple Dscam splice variants by individual cells. *Nature Genet*. 2004; 36:240–246. [PubMed: 14758360]
29. Lee CH, Herman T, Clandinin TR, Lee R, Zipursky SL. N-cadherin regulates target specificity in the *Drosophila* visual system. *Neuron*. 2001; 30:437–450. [PubMed: 11395005]
30. Lee T, Luo L. Mosaic analysis with a repressible cell marker (MARCM) for *Drosophila* neural development. *Trends Neurosci*. 2001; 24:251–254. [PubMed: 11311363]

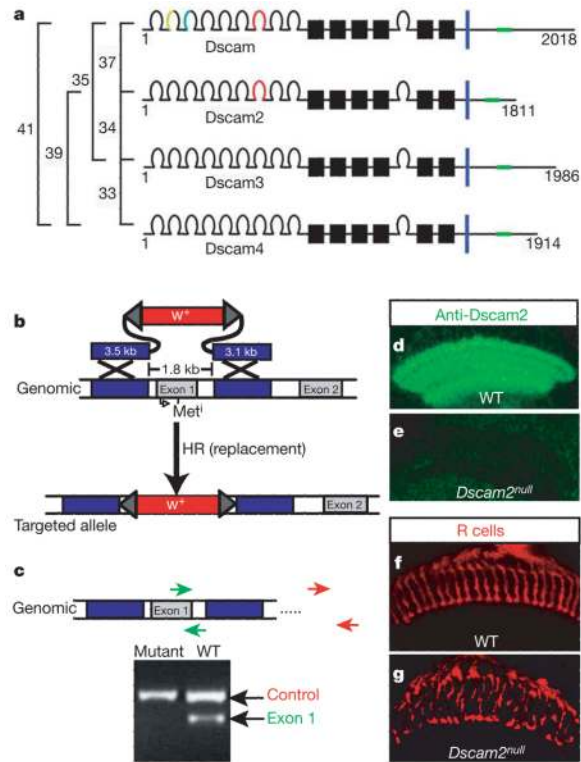


### Figure 1. *Dscam2* is required for visual system development

**a**, *Drosophila* *Dscam* family members. The percentage identity between the extracellular domains is shown at the left, and the number of amino acid residues in the protein at the right. *Dscam* isoforms differ within three immunoglobulin domains (coloured horseshoes). *Dscam2* has two isoforms differing at immunoglobulin domain 7 (red horseshoe). Immunoglobulin domains, horseshoes; FN domains, black boxes; transmembrane domains, blue bars. **b**, Homologous recombination (HR) scheme to knock out *Dscam2* (see Methods). kb, kilobases; w<sup>+</sup> indicates the *white* gene which is used as a marker to detect recombinants. **c**, Molecular verification of the targeting event by polymerase chain reaction. WT, wild type. **d**, **e**, *Dscam2* mutants are protein-null. The images show wild-type (**d**) and *Dscam2* mutant (**e**) pupal brains stained with a *Dscam2* antibody 40 h after puparium formation (APF). **f**, **g**, R7 and R8 projections in the medulla stained with monoclonal antibody 24B10 (red) are disorganized in adult *Dscam2* mutant brains. The projections of other neuronal classes were also disrupted (see Supplementary Fig. 1).



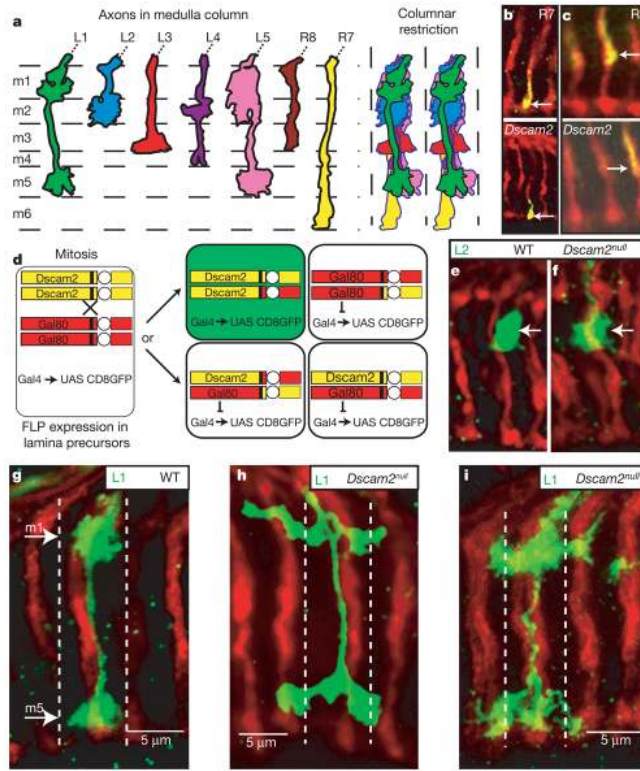


**Figure 2. *Dscam2* restricts L1 arbors to columns**  
**a**, Schematic of lamina neuron and R-cell projections in the medulla. Each cell targets to a specific layer (m1–m6, left) and is restricted to a single column (right). **b**, **c**, R7 and R8 do not require *Dscam2*. The terminals of mutant R7 (**b**) and mutant R8 (**c**) (yellow, bottom) in adult brains are indistinguishable from wild-type R7 and R8 (yellow, top). All R7 and R8 axons (red) are stained with monoclonal antibody 24B10 in this figure. **d**, MARCM scheme. A lamina-specific enhancer was used to drive FLP in lamina precursor cells. Homozygous mutant cells lacking the Gal80 repressor were labelled with actin-Gal4 and UAS-CD8GFP (green). **e**, **f**, L2 cells do not require *Dscam2*. Wild-type (**e**) and mutant (**f**) L2 terminals (green) were indistinguishable. **g–i**, L1 cells require *Dscam2* for columnar restriction. Wild-type L1 axons (**g**) arborized in the m1 and m5 layers of the medulla and were restricted to a single column (dashed lines). Mutant L1 cells (**h**, **i**) targeted to the correct layers, but their arbors were not restricted to a single column. Animals were analysed at about 70% APF in **e–i**.

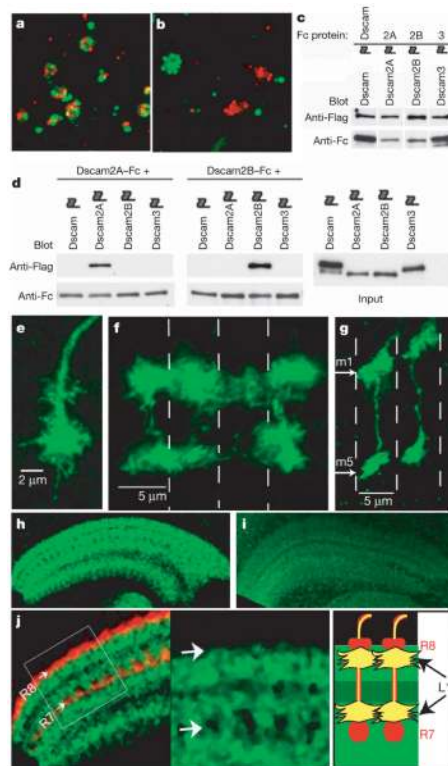


**Figure 3. Dscam2 binds homophilically and its expression is correlated with L1 arbor retraction during development**

**a, b**, Cell aggregation assay (see Methods). **a**, Control. Cells expressing Dscam2A (marked by co-expression of red fluorescent protein) mixed with cells expressing Dscam2A (marked by co-expression of green fluorescent protein). **b**, Cells expressing Dscam2A (red) and Dscam2B (green) segregate from one another, showing that homophilic interactions are isoform-specific. **c, d**, Pull-down assay. Dscam, Dscam2A, Dscam2B and Dscam3 ectodomain–Fc fusion proteins bound their cognate Flag-tagged full-length protein in extracts of transfected S2 cells (**c**; see Methods). **d**, Dscam2A or Dscam2B ectodomain–Fc fusion proteins bind to themselves but not other Dscam proteins. Right, inputs. The flag symbols in **c** and **d** indicate the Flag epitope. **e–g**, Wild-type L1 arbor development. At 30 h APF (**e**), wild-type L1 cells consist of a terminal growth cone and nascent m1 arbors. At about 40 h APF (**f**), L1 arbors in adjacent columns contact each other. The third column from the left does not contain a labelled L1 cell and this permits the detection of invading neurites from columns 2 and 4. At about 70 h APF (**g**), L1 processes are restricted to a single column. **h, i**, Dscam2 protein expression in the medulla during pupal development. Dscam2 expression peaks during the retraction phase of L1 development (40 h APF; **h**), and is then downregulated (70 h APF; **i**). **j**, Dscam2 distribution (green) is non-uniform at 40 h APF. Left, image also stained with monoclonal antibody 24B10 (red). Middle,  $\times 2.5$  magnification of the boxed region. Right, at this stage, L1 arbors reside immediately above R7 and immediately below R8 in layers with strong Dscam2 staining.

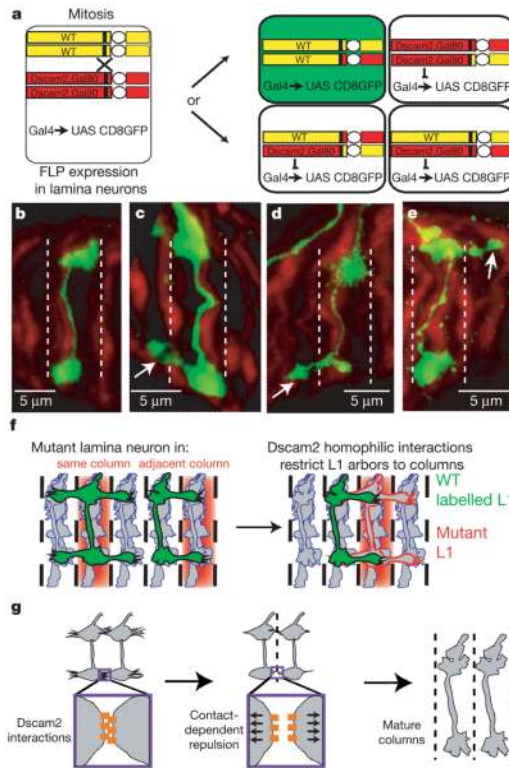


**Figure 4. *Dscam2* homophilic interactions are required for axonal tiling**  
**a**, Reverse MARCM scheme. The *Dscam2* mutation is on the Gal80-containing chromosome so that the wild-type, but not mutant, cells are labelled. **b**, A wild-type L1 neuron (green) in a wild-type background generated by MARCM (control). **c–e**, Non-autonomous tiling phenotypes in wild-type cells using the reverse MARCM technique. Note the unidirectional nature of the phenotype. R cells (red) are labelled with monoclonal antibody 24B10. **f**, Left, Possible outcomes of reverse MARCM. Non-autonomous phenotypes could arise from interactions with a *Dscam2* mutant cell in the same or an adjacent column. A requirement in the same column would generate a bidirectional phenotype, whereas a requirement in an adjacent column would generate a unidirectional phenotype. Right, Observed result and interpretation. The reverse MARCM phenotype is exclusively unidirectional (see also Supplementary Fig. 2), indicating that *Dscam2* homophilic interactions mediate repulsion. We propose this is due to a mutant ‘unlabelled’ L1 neuron (red) in the adjacent column. **g**, Model for columnar restriction of L1 arbors. Neurites from L1 cells in adjacent columns interact through *Dscam2* homophilic contacts. This generates a repulsive signal resulting in the retraction of neurites to their column of origin. It is important to note that if *Dscam2* expression is not restricted to L1 neurons in the layer, then isoform-specific or co-receptor-specific mechanisms may restrict *Dscam2* activity to L1 neurons within these layers.